Quantum Theory of Helium-4 Monolayers

H. W. Jackson

Scientific Laboratory, Ford Motor Company, Dearborn, Michigan 48121

(Received 3 October 1968)

A quantum theory of adsorbed, mobile monolayers of He[4] is developed. The formalism, which includes consideration of both the ground state and the excited states, is followed by numerical results for experimentally interesting examples.

I. INTRODUCTION

The behavior of an adsorbed He[4] monolayer can be analyzed simply when the particles are free to undergo fluid motion laterally. Strong interaction of the helium atoms with each other as well as with the substrate is assumed in the theory developed here, and small excursions of the adatoms normal to the plane of the surface are taken into account. In an effort to make our treatment fairly general while avoiding undue complication, we neglect the detailed structure of the substrate, in much the same spirit that one works with the jellium model of a solid. In brief, we will study a thin liquid film in a strong external field that is highly anisotropic in one direction, and focus attention mainly on the properties of its energy spectrum and eigenstates. A discussion of the formalism is followed by presentation of the results of numerical computation for experimentally interesting examples.

II. DESCRIPTION OF THE MODEL

The system of interest is composed of N He[4] atoms distributed over a square of area A in the x-z plane, where periodic boundary conditions are imposed in order to account for translational symmetry. There is a pairwise interaction of the Lennard-Jones (LJ) type,

$$V(r) = \alpha/r^{12} - \beta/r^6 \tag{1a}$$

$$= 4\epsilon \left[(\sigma/r)^{12} - (\sigma/r)^6 \right], \tag{1b}$$

which can be roughly characterized by a hard core, with diameter $d = 2.3$ Å, surrounded by a neighborhood of weak attraction at slightly greater distances. $W(y)$ is an anisotropic potential felt by each atom due to the substrate. The boundary conditions are that the wave functions vanish in the following regions:

$y \leq 0$,   simulates overlap of hard core of helium atom with hard core in the substrate,

$y \to \infty$,   bound surface layer.

For a basic two-particle Lennard-Jones potential between He[4] and a substrate of uniform density ρ, a straightforward calculation gives

$$W(y) = \pi\rho[\alpha/45(y+d)^9 - \beta/6(y+d)^3] . \tag{2}$$

The quantity d is the distance between helium and substrate when hard cores first make contact. Within narrow limits it is an adjustable parameter. In the numerical work of Sec. VIII, a somewhat different effective potential, corresponding to a substrate of bulk copper covered by a monolayer of argon, is used; it is displayed graphically in Fig. 3. For the present we proceed formally by adding in the kinetic energy to write a model Hamiltonian for the surface in the following way:

$$\mathcal{H} = \sum_{1 \leq i \leq N} -\frac{\hbar^2}{2m} \Delta_i$$

$$+ \sum_{1 \leq i < j \leq N} V(r_{ij}) + \sum_{1 \leq i \leq N} W(y_i). \tag{3}$$

III. THE MONOLAYER GROUND STATE

The ground-state wave function for the surface is assumed to have the following properties: (1) It is nondegenerate and therefore can be chosen real. (2) It is of one sign and can be chosen positive. (3) It satisfies the requirements of Bose statistics in the sense that it is symmetric in the particle coordinates.

Qualitatively, a wave function for a many-particle system can be described in words by stating how it assigns numbers to every arrangement of the atoms. Frequently considerable insight can be gained by identifying just the conditions of very high probability and some of those of very low. Feynman[1] used this approach in discussing He[4] bulk liquid, and we will simply adapt his technique to our situation. In the ground state, configurations of high-potential energy are improbable, and the kinetic energy is as small as possible consistent with this. These ideas can be made plausible

by applying a variational principle, in which the ground-state wave function is characterized by the property that it produces the minimum expectation value of the Hamiltonian. From this line of reasoning we infer that the ground-state wave function is small whenever hard cores overlap, since the potential energy is then high. To understand the role played by the kinetic energy, suppose that one atom moves in the cage formed by its neighbors, which are held fixed. Refer to Fig. 1 and look at the variation of $\psi_0(\vec{r}_1, \ldots, \vec{r}_N)$ as atom 2 travels on the line between 1 and 3. A very small value of ψ_0 is required by the potential considerations described above when 2 is close to 1 or 3. For intermediate positions, the curvature of the wave function, and in turn the contribution to the
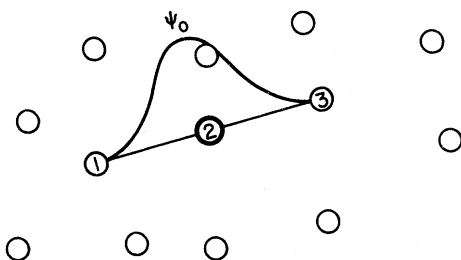

FIG. 1. Variation of the ground-state wave function ψ_0 as atom 2 moves in the cage formed by its neighbors, while all other atoms remain stationary.

kinetic energy, will be minimal if ψ_0 is of one sign and has a single peak that occurs near the midpoint between 1 and 3. This argument suggests that compression of the system increases its kinetic energy. On the other hand, expansion requires that work be done against the attractive van der Waals forces. Equilibrium is reached when these two effects are balanced, and the most likely configurations are uniform distributions with each particle near the center of its cage.

This description should be reasonably accurate for the ground-state wave function in the plane of the surface. The dependence on the normal coordinate, y, can be studied most easily when the adatoms are tightly bound. In this case any motion in the y direction is strongly regulated by the potential $\sum_i W(y_i)$, and $|\psi_0|$ is large only when the adsorbed atoms are very close to the substrate. An indirect consequence of this vertical confinement is that the projections of the atomic hard cores on the x-z plane hardly ever overlap. Under these circumstances little error is introduced in matrix elements of the potential, particularly with respect to the low-energy states of the system, if $V(r_{ij})$ is replaced by $V(\rho_{ij})$, where $\vec{\rho}$ is the com-

ponent of $\vec{r}$ along the surface. This same procedure should give a good approximation even in weakly bound systems when the average lateral distance between atoms is large, i. e., for conditions of low coverage. The Hamiltonian now divides in a natural way into zeroth order and perturbing parts.

$$\mathcal{H} = \mathcal{H}_0 + \mathcal{H}_1, \tag{4}$$

$$\mathcal{H}_0 = \sum_{1 \leq i \leq N} -\frac{\hbar^2}{2m}\Delta_i$$

$$+ \sum_{1 \leq i < j \leq N} V(\rho_{ij}) + \sum_{1 \leq i \leq N} W(y_i), \tag{5}$$

$$\mathcal{H}_1 = \sum_{1 \leq i < j \leq N} [V(r_{ij}) - V(\rho_{ij})]. \tag{6}$$

The effect of $\mathcal{H}_1$ can be evaluated only after the zeroth-order problem has been completely solved. We intend to treat this perturbation in detail in a later paper, but for now our concern is limited to $\mathcal{H}_0$, which can be decomposed into a parallel part, $\mathcal{H}_{0P}$, that involves only the components of $\vec{\rho}_i$, and a normal part $\mathcal{H}_{0N}$ that contains only the y_i. Explicitly

$$\mathcal{H}_0 = \mathcal{H}_{0P} + \mathcal{H}_{0N}, \tag{7}$$

where $\mathcal{H}_{0P} = \sum_{1 \leq i \leq N} \left[-\frac{\hbar^2}{2m}\left(\frac{\partial^2}{\partial x_i^2} + \frac{\partial^2}{\partial z_i^2}\right)\right]$

$$+ \sum_{1 \leq i < j \leq N} V(\rho_{ij}), \tag{8}$$

and $\mathcal{H}_{0N} = \sum_{1 \leq i \leq N} \left[-\frac{\hbar^2}{2m}\frac{\partial^2}{\partial y_i^2}\right] + \sum_{1 \leq i \leq N} W(y_i)$

$$= \sum_{1 \leq i \leq N} h(y_i). \tag{9}$$

An eigenfunction of $\mathcal{H}_0$ can be written as a product of normal and parallel parts. In particular, for the ground state, we have

$$\psi_0(\vec{r}_1, \ldots, \vec{r}_N) = \varphi_0(y_1)\varphi_0(y_2)\cdots$$

$$\times \varphi_0(y_N)\chi(\vec{\rho}_1, \vec{\rho}_2, \ldots, \vec{\rho}_N), \tag{10}$$

and $\mathcal{H}_0\psi_0 = \mathcal{E}_0\psi_0$ \hfill (11)

with $\mathcal{E}_0 = N\mathcal{E}_{0N} + \mathcal{E}_{0P}$. \hfill (12)

Here it is understood that φ_0 and χ are solutions of

$$h(y_i)\varphi_0(y_i) = \mathscr{E}_{0N}\varphi_0(y_i) ,$$ (13)

and $\mathscr{K}_{0P}\chi(\vec{\rho}_1, \vec{\rho}_2, \dots, \vec{\rho}_N) = \mathscr{E}_{0P}\chi(\vec{\rho}_1, \vec{\rho}_2, \dots, \vec{\rho}_N) ,$ (14)

respectively, where $\mathscr{E}_{0N}$ and $\mathscr{E}_{0P}$ are the lowest eigenvalues consistent with the boundary conditions in Sec. II, and χ is symmetric in its arguments. For future reference we remark that $\varphi_1(y_i)$ is the first excited state of $h(y_i)$, with energy $\mathscr{E}_{0N} + \mathscr{E}_{1N}$.

IV. WAVE FUNCTIONS FOR EXCITED STATES

The operator for the parallel component of linear momentum commutes with $\mathscr{K}_0$, and therefore they can be simultaneously diagonalized. When the reference frame is chosen so that χ has vanishing parallel momentum, one can immediately write down a large set of excited-state wave functions with this same property. For example,

$$\psi_1 = \sum_{1 \le l \le N} \frac{\varphi_1(y_l)}{\varphi_0(y_l)} \psi_0$$ (15)

qualifies as such and belongs to the energy eigenvalue $\mathscr{E}_0 + \mathscr{E}_{1N}$. Others are of the form

$$\psi = \sum_\nu P_\nu \frac{\varphi_a(y_1)}{\varphi_0(y_1)} \cdots \frac{\varphi_r(y_N)}{\varphi_0(y_N)} \psi_0 ,$$ (16)

where ν ranges over all distinct permutations of the state labels included in the product.

A more interesting problem is to find approximate energy eigenfunctions for which the momentum is nonzero. In this paper, attention is directed only to the simplest cases, where a single excitation is present. It is shown that a surface density fluctuation, which we call a longitudinal surfon, is described by the wave function

$$\psi_{\vec{k}}^L = \sum_{1 \le l \le N} e^{i\vec{k} \cdot \vec{\rho}_l} \psi_0 ,$$ (17)

where $\vec{k}$ is in the plane of the surface, and that a second kind of surfon, a transverse wave, is described by

$$\psi_{\vec{k}}^{T1} = \sum_{1 \le l \le N} e^{i\vec{k} \cdot \vec{\rho}_l} \frac{\varphi_1(y_l)}{\varphi_0(y_l)} \psi_0 .$$ (18)

Extension of this theory to account for multiple excitations can very likely be carried out by use of broad wave packets, or perhaps by direct cal-

culation with the aid of a generalized superposition approximation for high-order distribution functions. Both of these methods have been successfully applied to superfluid helium.[2,3]

Longitudinal Surfons. The physical situation represented by $\psi_{\vec{k}}^L$ is essentially the same as that discussed by Feynman for the bulk liquid. It may be worthwhile to repeat and elaborate on his discussion in order to pave the way for analyzing $\psi_{\vec{k}}^{T1}$, which is slightly more complicated.

The wave function $\psi_{\vec{k}}^L$ is small when *any* atom is either very far from or close to the substrate; this is guaranteed by the factors of φ_0 in ψ_0. In order to exhibit other properties of $\psi_{\vec{k}}^L$, we choose an origin at one corner of the normalization square, and look at a typical cross section in the x-y plane. At first take $\vec{k}$ in the x direction, and then consider

$$\mathrm{Re}\psi_{\vec{k}}^L = \sum_{1 \le l \le N} \psi_0 \cos kx_l .$$ (19)

When at least two atoms are squeezed together tightly, $\mathrm{Re}\psi_{\vec{k}}^L$ is small because of the χ factor in ψ_0. In contrast to this, for a uniform spacing, χ is close to its maximum value; but then there are as many atoms in positive as negative regions along the cosine curve, and $\mathrm{Re}\psi_{\vec{k}}^L$ is now small due to the sum over l. However, for particular configurations with alternate regions of slight compression and rarefaction repeating with wavelength $\lambda = 2\pi/k$, as shown in Fig. 2(a), χ is still
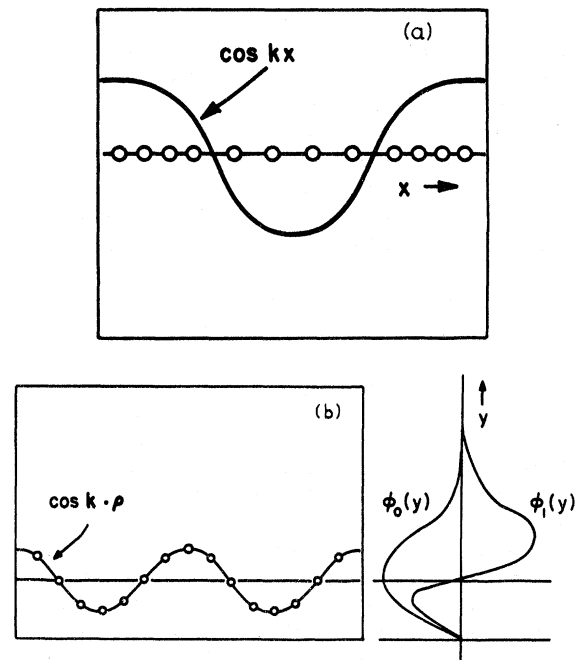

FIG. 2. (a) Condition of high probability in $\psi_{\vec{k}}^L$.
(b) Condition of high probability in $\psi_{\vec{k}}^{T1}$.

large, and the cancellation is incomplete because more atoms are in positive than in negative intervals, so that $\text{Re}\psi_{\vec{k}}^{L}$ is large. For these same arrangements it is easy to see that $\text{Im}\psi_{\vec{k}}^{L}$ is small. Furthermore, the fact that $\psi_{\vec{k}}^{L}$ is an eigenfunction of the parallel momentum operator implies that

$$e^{i\vec{k}\cdot\vec{a}}\psi_{\vec{k}}^{L}(\vec{r}_1-\vec{a},\vec{r}_2-\vec{a},\ldots,\vec{r}_N-\vec{a})$$

$$=\psi_{\vec{k}}^{L}(\vec{r}_1,\vec{r}_2,\ldots,\vec{r}_N)\ ,\tag{20}$$

where $\vec{a}$ is an arbitrary vector in the plane of the surface. Here, of course, we have assumed extension of the system to infinity by the use of periodic boundary conditions and appropriate identification of congruent particles. Equation (20) together with the discussion preceding it implies that $|\psi_{\vec{k}}^{L}|^2$, the probability density for a surfon, is large whenever density fluctuations occur with wavelength $\lambda=2\pi/k$ in the direction of $\vec{k}$, and that this is independent of the origin of coordinates. Clearly these longitudinal surfons are just the two-dimensional version of acoustic phonons.

So far we have implicitly assumed that $\lambda=2\pi/k$ is much larger than the average interatomic spacing, so that many particles fall into each cycle. If this is not the case, our qualitative interpretation of the wave function $\psi_{\vec{k}}^{L}$ is not correct. To examine the situation for small λ, suppose that it is equal to the cube root of the mean atomic volume. Then taking a typical cross-sectional view as before, one sees that the largest probability density occurs when each atom is at the center of the cage formed by its neighbors, but that the curvature of the wave function is greater than that of the ground state as an atom roams about in its enclosure. This suggests that a short-wavelength longitudinal surfon corresponds to a state in which each atom is excited in its own cage and moves in such a way as to produce a net current in the direction of $\vec{k}$.

Transverse Surfons. To see that the function $\psi_{\vec{k}}^{T1}$ in Eq. (18) does indeed describe a transverse wave, again look at a cross section of the surface. At first consider a situation in which all atoms are at the same height y and distributed uniformly in the x-z plane. Then provided that the wavelength $\lambda=2\pi/k$ is much greater than the average atomic spacing, the wave function is almost zero for the same reason as in the longitudinal case. One can easily find other essentially null arrangements. After some reflection, one also discovers the most probable conditions. This is the matter to be discussed now. For definiteness, refer to Fig. 4 and notice that $\varphi_1(y)$ has a node in a region where $\varphi_0(y)$ is large. (The functions φ_0 and φ_1 have been sketched at the right of Fig. 2(b) for ready reference.) In gener-

al one expects this qualitative behavior because of normalization and orthogonality constraints. Now suppose the atoms are distributed as in Fig. 2(b). The function χ is near its maximum value and each factor of φ_0 is large for this configuration. We ask, what is the result of the operator

$$\sum_{1\le l\le N} e^{i\vec{k}\cdot\vec{\rho}l}[\varphi_1(y_l)/\varphi_0(y_l)]$$

acting on ψ_0? The real part of $\psi_{\vec{k}}^{T1}$, namely,

$$\text{Re}\psi_{\vec{k}}^{T1}=\sum_{1\le l\le N}\cos\vec{k}\cdot\vec{\rho}_l\ \frac{\varphi_1(y_l)}{\varphi_0(y_l)}\ \psi_0\ ,\tag{21}$$

consists of terms which, for the conditions of Fig. 2(b), are all negative because the factor $\cos\vec{k}\cdot\vec{\rho}_l$ always has the opposite sign from $\varphi_1(y_l)/\varphi_0(y_l)$. This implies that there is no cancellation in the sum over l, and $|\text{Re}\psi_{\vec{k}}^{T1}|$ is large. Furthermore, $|\text{Im}\psi_{\vec{k}}^{T1}|$ is negligible for this arrangement. One can easily supply the details which show that $|\psi_{\vec{k}}^{T1}|^2$ is large for all translations of the configuration under consideration, and thereby convince himself that $\psi_{\vec{k}}^{T1}$ does in reality represent a transverse wave, independent of the choice of coordinate system.

V. DEFINITIONS AND FORMULAS

To the equations already developed, we add the following formulas and definitions to provide a basis for the mathematical analysis in subsequent sections.

Eigenvalue-eigenfunction equation for single-particle excited states in the normal direction:

$$h(y)\varphi_i(y)=(\mathcal{E}_{0N}+\mathcal{E}_{iN})\varphi_i(y)\ ,\ i=1,2,\ldots,r\ .$$

It is assumed that there are r-bound excited states; of course, the number is dependent on the depth and range of $W(y)$, and in particular instances there may be none.

Zeroth-order transverse surfon wave function (ith branch):

$$\psi_{\vec{k}}^{Ti}=\sum_{1\le l\le N}e^{i\vec{k}\cdot\vec{\rho}l}\ \frac{\varphi_i(y_l)}{\varphi_0(y_l)}\ \psi_0\ .\tag{23}$$

Pair distribution function in a plane surface:

$$s^2\gamma(\rho_{12})=N(N-1)\int\chi^2 d\vec{\rho}_3\cdots d\vec{\rho}_N\ ,\tag{24}$$

where $s=N/A$ is the average number of atoms per unit area.

Surface structure function for a plane system:

$$\sigma(k)=1+s\int e^{i\vec{k}\cdot\vec{\rho}}[\gamma(\rho)-1]d\vec{\rho}\ .\tag{25}$$

Normalization conditions:

$$\int_0^\infty \varphi_i^*(y)\varphi_i(y)dy = 1, \quad i = 0, 1, 2, \ldots, r$$

$$\int \chi^2(\vec{\rho}_1, \ldots, \vec{\rho}_N)d\vec{\rho}_1 \cdots d\vec{\rho}_N = 1 . \tag{26}$$

In Eqs. (24) and (25) we have introduced direct analogs of quantities for three dimensional systems.

VI. ORTHOGONALITY AND NORMALIZATION OF SURFON WAVE FUNCTIONS

The mutual orthogonality of $\psi_{\vec{k}}^L$, $\psi_{\vec{k}}^{Ti}$, and ψ_0 will now be proved. Since the parallel momentum of $\psi_{\vec{k}}^L$ and $\psi_{\vec{k}}^{Ti}$ is different from zero, we have immediately that

$$\langle \psi_{\vec{k}}^L | 1 | \psi_0 \rangle = \int \psi_{\vec{k}}^{L*} \psi_0 d\vec{r}_1 \cdots d\vec{r}_N = 0 , \tag{28}$$

and

$$\langle \psi_{\vec{k}}^{Ti} | 1 | \psi_0 \rangle = \int \psi_{\vec{k}}^{Ti*} \psi_0 d\vec{r}_1 \cdots d\vec{r}_N = 0 . \tag{29}$$

To show that $\psi_{\vec{k}}^L$ is orthogonal to $\psi_{\vec{k}}^{Ti}$, write

$$\langle \psi_{\vec{k}}^L | 1 | \psi_{\vec{k}}^{Ti} \rangle = \int \psi_{\vec{k}}^{L*} \psi_{\vec{k}}^{Ti} d\vec{r}_1 \cdots d\vec{r}_N$$

$$= \sum_{l,j} \int e^{i\vec{k}\cdot(\vec{\rho}_l - \vec{\rho}_j)} \chi^2 d\vec{\rho}_1 \cdots d\vec{\rho}_N$$

$$\times \int [\varphi_0(y_1) \cdots \varphi_0(y_l) \cdots \varphi_0(y_N)]$$

$$\times [\varphi_0(y_1) \cdots \varphi_i(y_l) \cdots \varphi_0(y_N)]$$

$$\times dy_1 \cdots dy_N = 0 . \tag{30}$$

The last step follows from the presence of a factor

$$\int \varphi_0(y_l)\varphi_i(y_l)dy_l = 0 , \quad i \neq 0 \tag{31}$$

in each term.

The diagonal matrix element of the identity for a longitudinal surfon state is

$$\langle \psi_{\vec{k}}^L | 1 | \psi_{\vec{k}}^L \rangle = N[\sigma(k) + (2\pi)^2 s\delta(\vec{k})] . \tag{32}$$

This simple answer appears only when one neglects edge effects.

The matrix elements of the identity for transverse surfon states are found in a few short steps to be

$$\langle \psi_{\vec{k}}^{Ti} | 1 | \psi_{\vec{k}}^{Tj} \rangle = N\delta_{ij} . \tag{33}$$

In view of Eqs. (32) and (33), we see that the normalized surfon wave functions are, for $k \neq 0$,

$$\Phi_{\vec{k}}^L = [N\sigma(k)]^{-\frac{1}{2}} \sum_{1 \leq l \leq N} e^{i\vec{k}\cdot\vec{\rho}_l} \psi_0 , \tag{34}$$

$$\Phi_{\vec{k}}^{Ti} = N^{-\frac{1}{2}} \sum_{1 \leq l \leq N} e^{i\vec{k}\cdot\vec{\rho}_l} \frac{\varphi_i(y_l)}{\varphi_0(y_l)} \psi_0 . \tag{35}$$

VII. MATRIX ELEMENTS OF THE ZEROTH-ORDER HAMILTONIAN

Matrix elements of $\mathcal{K}_0$ with respect to wave functions of the type

$$\psi_a = \sum_{1 \leq l \leq N} f_a(\vec{r}_l)\psi_0 \equiv F_a\psi_0 \tag{36}$$

are especially easy to evaluate. To show this in detail, we first write

$$\langle \psi_a | \mathcal{K}_0 - \mathcal{E}_0 | \psi_b \rangle = \int \psi_a^* (\mathcal{K}_0 - \mathcal{E}_0)\psi_b d\tau$$

$$= \int F_a^*\psi_0 \left[\sum_{1 \leq i \leq N} \left(-\frac{\hbar^2}{2m} \Delta_i \right) \right.$$

$$+ \sum_{1 \leq i < j \leq N} V(\rho_{ij}) + \sum_{1 \leq i \leq N} W(y_i) - \mathcal{E}_0 \left] F_b\psi_0 d\tau , \right.$$
$$\tag{37}$$

where $d\tau = d\vec{r}_1 \cdots d\vec{r}_N$. \hfill (38)

The identity

$$\Delta_i F_b\psi_0 = (\Delta_i F_b)\psi_0 + F_b\Delta_i\psi_0 + 2\vec{\nabla}_i\psi_0 \cdot \vec{\nabla}_i F_b , \tag{39}$$

together with the eigenvalue equation

$$(\mathcal{K}_0 - \mathcal{E}_0)\psi_0 = 0 , \tag{40}$$

enable us to express Eq. (37) as

$$\langle \psi_a | \mathcal{K}_0 - \mathcal{E}_0 | \psi_b \rangle = \sum_{1 \leq i \leq N} \left(-\frac{\hbar^2}{2m} \right.$$

$$\times \int F_a^* (\psi_0^2 \Delta_i F_b + \vec{\nabla}_i\psi_0^2 \cdot \vec{\nabla}_i F_b)d\tau \left. \right) . \tag{41}$$

Next we introduce the relation

$$\vec{\nabla}_i \cdot (\psi_0^2 F_a^* \vec{\nabla}_i F_b) = \psi_0^2 \vec{\nabla}_i F_a^* \cdot \vec{\nabla}_i F_b$$

$$+ \psi_0^2 F_a^* \cdot \Delta_i F_b + F_a^* \vec{\nabla}_i F_b \cdot \vec{\nabla}_i\psi_0^2 , \tag{42}$$

to further reduce Eq. (41).

$$\langle\psi_a|\mathcal{3C}_0 - \mathcal{E}_0|\psi_b\rangle = \sum_{1\leq i \leq N} \left(-\frac{\hbar^2}{2m}\right)$$

$$\times\left[\int\vec{\nabla}_i\cdot(\psi_0{}^2 F_a{}^*\vec{\nabla}_i F_b)d\tau - \int(\vec{\nabla}_i F_a{}^*\cdot\vec{\nabla}_i F_b)\psi_0{}^2 d\tau\right].$$
(43)

With the aid of Gauss's theorem one can convert the first term in the last line to a surface integral which vanishes under the specified boundary conditions. Hence

$$\langle\psi_a|\mathcal{3C}_0 - \mathcal{E}_0|\psi_b\rangle$$

$$=\frac{\hbar^2}{2m}\sum_{1\leq i \leq N}\int(\vec{\nabla}_i F_a{}^*\cdot\vec{\nabla}_i F_b)\psi_0{}^2 d\tau.$$
(44)

Because of the symmetry of $\psi_0{}^2$, F_a, and F_b in the particle coordinates, each term in the sum has the same value, and Eq. (44) can be written as

$$\langle\psi_a|\mathcal{3C}_0 - \mathcal{E}_0|\psi_b\rangle$$

$$=(\hbar^2/2m)N\int\psi_0{}^2\vec{\nabla}_1 F_a{}^*\cdot\vec{\nabla}_1 F_b d\tau.$$
(45)

Now we can work out the matrix elements of $\mathcal{3C}_0 - \mathcal{E}_0$ between single surfon states. Straightforward application of Eq. (45) gives

$$\langle\Phi_{\vec{k}}{}^L|\mathcal{3C}_0 - \mathcal{E}_0|\Phi_{\vec{k}}{}^{Ti}\rangle = 0,$$
(46)

$$\langle\Phi_{\vec{k}}{}^L|\mathcal{3C}_0 - \mathcal{E}_0|\Phi_{\vec{k}}{}^L\rangle = \frac{\hbar^2 k^2}{2m\sigma(k)} = \mathcal{E}_L(k),$$
(47)

$$\langle\Phi_{\vec{k}}{}^{Ti}|\mathcal{3C}_0 - \mathcal{E}_0|\Phi_{\vec{k}}{}^{Tj}\rangle = \left(\frac{\hbar^2 k^2}{2m} + \mathcal{E}_{iN}\right)\delta_{ij}.$$
(48)

To derive the last equation we have used the relation

$$\mathcal{E}_{iN}\delta_{ij} = \int_0^\infty \varphi_i(y)[h(y) - \mathcal{E}_{0N}]\varphi_j(y)dy$$
(49)

$$=\frac{\hbar^2}{2m}\int_0^\infty \varphi_0{}^2(y)\left(\frac{d}{dy}\frac{\varphi_i(y)}{\varphi_0(y)}\right)\left(\frac{d}{dy}\frac{\varphi_j(y)}{\varphi_0(y)}\right)dy,$$

which is essentially just a special case of Eq. (45). Of course, Eq. (48) can also be established directly without the aid of Eqs. (45) and (49). The set of Eqs. (46)–(48) show that the zeroth-order Hamiltonian is diagonal in the surfon representation, within the restricted manifold of states spanned by single-excitation wave functions.

The shape of the longitudinal excitation spectrum can be found only after $\sigma(k)$ is known. One way to arrive at a theoretical value for this latter quantity is to use a variational procedure, starting with, say, a Jastrow form for χ, i.e.,

$$\chi(\vec{\rho}_1,\ldots,\vec{\rho}_N) = \prod_{1\leq i<j \leq N} e^{\frac{1}{2}U(\rho_{ij})}.$$
(50)

Here $U(\rho)$ is a two-particle correlation function for a two-dimensional system, and may be approximated and parametrized by taking the three-dimensional analog as a guide. For the model we are considering, $\sigma(k)$ will depend only on the density of the adsorbed atoms and the interaction between them, but not on the potential $W(y)$. Be that as it may, $W(y)$ plays a dominant role in fixing the values of the $\mathcal{E}_{iN}$. Therefore by varying the materials in the substrate, one will change the $\mathcal{E}_{iN}$ but not $\mathcal{E}_L$. Consequently carefully planned experiments should be able to probe the dependence on parallel and normal coordinates separately. This is discussed in the next section.

In the absence of definite knowledge of $\sigma(k)$, we submit the following description as a reasonable guess. It seems likely that, at least at moderately high areal densities, $\sigma(k)$ will roughly resemble $S(k)$ for the three-dimensional liquid. Then the zeroth-order longitudinal energy spectrum will have a linear phonon character for small wave vectors, which is consistent with Debye theory, and perhaps a rotonlike gap further out. The critical parameters consisting of the phonon velocity and the roton gap, location, and curvature may, of course, be quite different from those in the three-dimensional case.

VIII. NUMERICAL RESULTS

Before calculating the spectrum of the transverse modes, one must find the potential $W(y)$. Bardeen[4] has shown theoretically that a neutral atom distance y above a metallic surface feels an attractive potential given by

$$W_M(y) = -\gamma/y^3.$$
(51)

The value of γ for a helium atom over copper is 51.6×10^{-14} erg cm^3; this number was deduced from a result computed by Schiff and quoted by Atkins.[5]

The interaction between a pair of noble gas atoms, one of which is helium, should be accurately described by a Lennard-Jones potential of the form in Eq. (1). Since the parameters ϵ and σ have not been measured directly for atoms of different species, we have used interpolation formulas recommended by Hirschfelder, Curtiss, and Bird,[6] namely,

TABLE I. Properties of noble-gas elements. The Lennard–Jones parameters are based on the data of Ref. 6.

Material	ϵ/K_B (°K)	σ (Å)	d (Å)	l (Å)	s (Å^{-2})
He	10.22	2.556	2.300	· · ·	· · ·
Ne	35.60	2.749	· · ·	· · ·	0.105
Ar	119.8	3.405	· · ·	· · ·	0.0685
Kr	171	3.60	· · ·	· · ·	0.0613
Xe	221	4.100	· · ·	· · ·	0.0472
He–Ne	19.1	2.652	2.387	3.62	· · ·
He–Ar	35.0	2.980	2.682	4.21	· · ·
He–Kr	42.0	3.078	2.77	4.39	· · ·
He–Xe	47.5	3.328	2.995	4.84	· · ·

$$\sigma_{\alpha\beta} = \tfrac{1}{2}(\sigma_\alpha + \sigma_\beta), \qquad (52)$$

$$\text{and } \epsilon_{\alpha\beta} = (\epsilon_\alpha \epsilon_\beta)^{1/2}, \qquad (53)$$

where the single subscript refers to atoms of a given element, and the double subscript to the heterogeneous pairs. The values adopted in our work are based on data given in Ref. 6, page 1110, and are shown in Table I. When the noble-gas (NG) substrate is distributed uniformly with areal density s over a plane, the net attractive potential for a helium atom is

$$W_{NG}(y) = 2\pi s \left(\tfrac{1}{10} \alpha / y^{10} - \tfrac{1}{4} \beta / y^4 \right). \qquad (54)$$

The assumption of uniformity of the monolayer is reasonable only when the adatom is not too close; otherwise correlations between helium and substrate particles become important. To bypass difficulties arising in this way, we make the approximation that the helium stops when hard cores meet with the atomic centers a distance d apart. The choice of d is somewhat arbitrary, but we have taken it to be 0.9σ. The value of s for argon was computed from the data of McCormick, Goodstein, and Dash.[7] Under the assumption that the

area per atom is inversely proportional to the square of the Lennard-Jones parameter σ, s was calculated for the other noble gases. The results are given in Table I. Translation of the origin of the y coordinate to coincide with the boundary condition described above requires that we replace y by $(y + l)$ in Eq. (51), where

$$l = 0.9(\sigma_{NG} + 0.5\sigma_{He}), \qquad (55)$$

and σ_{NG} is the LJ parameter for the relevant noble gas. The total effective potential between a helium atom and the substrate is

$$W(y) = -\gamma / (y + l)^3$$
$$+ 2\pi s \left[\tfrac{1}{10} \alpha / (y + d)^{10} - \tfrac{1}{4} \beta / (y + d)^4 \right], \qquad (56)$$

which is plotted in Fig. 3.

The eigenvalues and eigenfunctions of $h(y)$, for a single-particle subject to the potential $W(y)$, were computed by numerical methods. Basically the procedure consisted of replacing the differential equation by a difference equation and then solving the latter. The grid used in this conversion was $\Delta k = 0.2$ Å^{-1}, which introduced errors of about 5%. This estimate is based on comparison
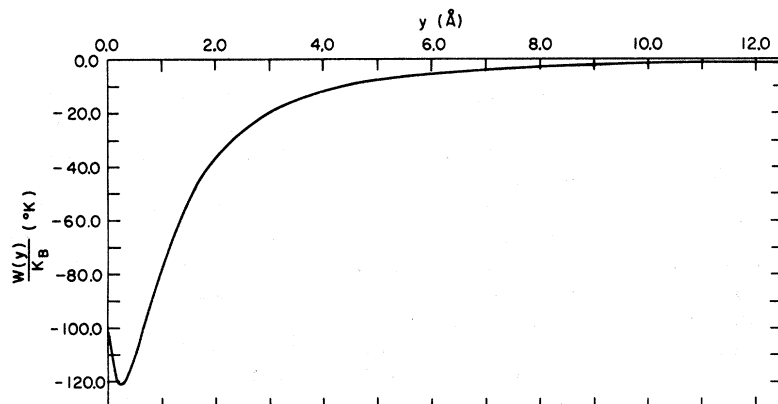

FIG. 3. Anisotropic potential for helium atom over substrate of bulk copper covered by argon monolayer.

with calculations for special cases with a grid of 0.1 Å⁻¹. The wave function was forced to vanish at 20.2 Å⁻¹ as an approximation to the boundary condition at infinity. This produces some uncertainty in the number of bound states since the energy eigenvalues are typically closely spaced near zero. For the cases studied we feel that only the last bound state is in doubt. The lowest four eigenvalues were consistently found to be quite insensitive to the choice of 20.2 Å⁻¹ as an upper limit. The eigenvalues for several different situations are listed in Table II. The computed ground-state

TABLE II. Bound-state eigenvalues of $h(y)$, the Hamiltonian for a single He⁴ atom in the y direction. The substrate is bulk copper covered by a monolayer of the noble-gas element indicated.

(°K)	Ne	Ar	Kr	Xe
$\mathcal{E}_{ON}/K_B$	-66.25	-73.94	-82.67	-80.18
$(\mathcal{E}_{ON}+\mathcal{E}_{1N})/K_B$	-27.47	-32.64	-38.20	-38.15
$(\mathcal{E}_{ON}+\mathcal{E}_{2N})/K_B$	-10.79	-13.35	-16.34	-16.72
$(\mathcal{E}_{ON}+\mathcal{E}_{3N})/K_B$	-3.79	-4.85	-6.21	-6.50
$(\mathcal{E}_{ON}+\mathcal{E}_{4N})/K_B$	-1.11	-1.48	-2.01	-2.14
$(\mathcal{E}_{ON}+\mathcal{E}_{5N})/K_B$	-0.05	-0.24	-0.46	-0.51

energy of a helium atom for a substrate of bulk copper covered by an argon monolayer given in the table is equivalent to 131.6 cal/mole. At high coverage the lateral interactions will make the binding energy somewhat greater than this, but the total will undoubtedly still be compatible with the determination that the energy of adsorption is less than 200 cal/mole, made by McCormick *et al.*

The eigenfunctions of $h(y)$ for the Cu-Ar substrate are shown in Fig. 4. One can see that the

helium monolayer in the ground state is localized within about 2 Å of the argon surface, and extends out only a few more angstroms for the first two excited states. Hence the tight-binding approximation is well suited to this problem. The eigenfunctions for the remaining cases have also been computed and are not much different from those shown in the figure.

If we treat the surfons as elementary excitations obeying Bose statistics, the heat capacity per unit area at constant coverage is

$$C_a = \frac{1}{2\pi k_B T^2} \sum_\alpha \int_0^\infty \frac{k\,dk\,\mathcal{E}_{\vec{k},\alpha}{}^2 \exp(\mathcal{E}_{\vec{k},\alpha}/k_B T)}{[\exp(\mathcal{E}_{\vec{k},\alpha}/k_B T)-1]^2}, \quad (57)$$

where α ranges over all branches of the energy spectrum.

Until $\sigma(k)$ is known in detail, we cannot compute the total heat capacity, but the contribution from the transverse modes has been evaluated. For ease of computation, Eq. (57) was transformed to

$$C_a = KT \sum_i \int_{x_0}^\infty \frac{x^2 e^x}{(e^x-1)^2}\,dx \text{ erg/}m^2, \quad (58)$$

where $K = 3.136 \times 10^{10}$ and $x_0 = \mathcal{E}_{iN}/k_B T$. To find the specific heat in cal/mole one must multiply C_a by the area (in m²) covered by a mole of adsorbed helium. The curves for different substrates are shown in Fig. 5.

Since for fixed coverage of helium the substrate does not influence the longitudinal modes, the difference in the total specific heat for all cases
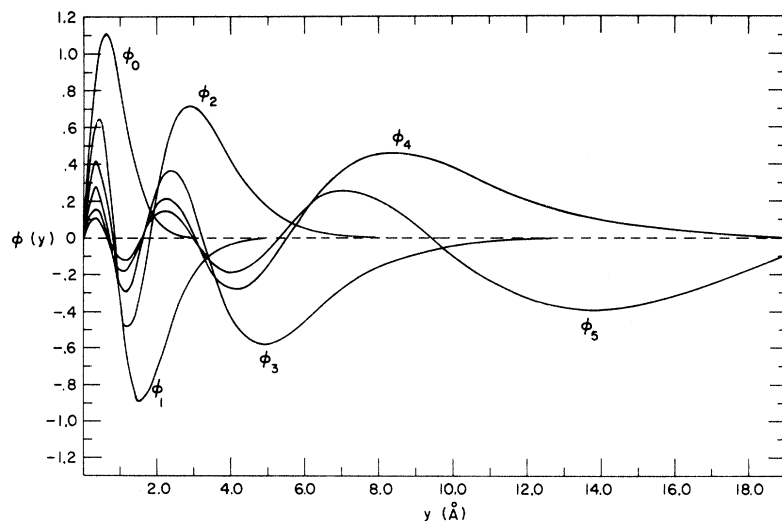

FIG. 4. Bound-state eigenfunction of $h(y)$, the Hamiltonian for a single He⁴ atom in the y direction. The substrate is bulk copper covered by an argon monolayer.

should be the same as that for the transverse modes alone. Although the approximations and uncertainties in our treatment may lead to errors of about 10 or 15%, we feel that the relative ordering of the specific heat curves is still correct.

Some experimental data for total specific heat, based on the high-coverage case of Ref. 7, is shown in Fig. 5. The area per atom here is 14.0 Å². A parabolic form was fit to the observed points below 3°K, and we have extrapolated that curve to high temperatures. Comparing it with our results, one recognizes that below 6°K the thermodynamic properties are completely dominated by the longitudinal modes, but that the transverse modes become increasingly important as the temperature rises. Of course, any experiment designed to observe this effect must take into account desorbing tendencies above about 10°K.
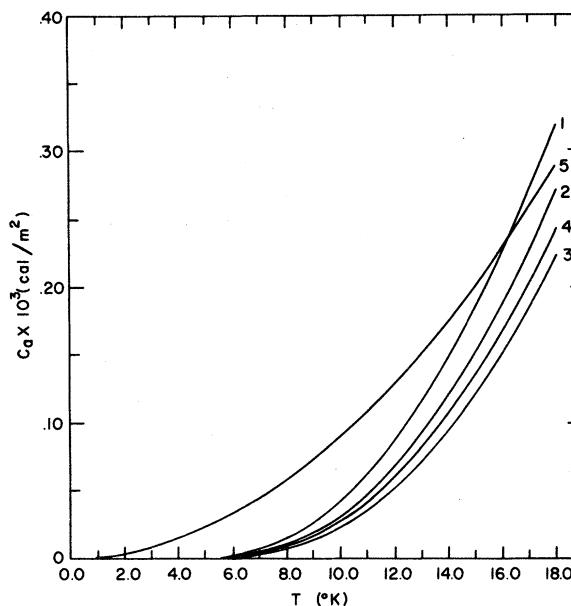

FIG. 5. Heat capacity per unit area at constant coverage for He[4] monolayer over a substrate of bulk copper covered by a single layer of noble-gas atoms as follows: (1) neon, (2) argon, (3) krypton, (4) xenon, and (5) argon. Curves 1–4 are for contributions from transverse modes only. Curve 5 is the total heat capacity deduced from experimental measurements below 3°K for an Ar–Cu substrate. (See text for details.)

ACKNOWLEDGMENT

[1] R. P. Feynman, Phys. Rev. 91, 1301 (1953).

[2] R. P. Feynman, Phys. Rev. 94, 262 (1954).

[3] H. W. Jackson and E. Feenberg, Ann. Phys. (N. Y.) 15, 266 (1961).

[4] J. Bardeen, Phys. Rev. 58, 727 (1940).

[5] K. R. Atkins, Liquid Helium (Cambridge University Press, Cambridge, England, 1959), p. 225.

[6] J. D. Hirschfelder, C. F. Curtiss, and R. B. Bird, Molecular Theory of Gases and Liquids (John Wiley & Sons, Inc., New York, 1954), p. 222.

[7] W. D. McCormick, D. L. Goodstein, and J. G. Dash, Phys. Rev. 168, 249 (1968).